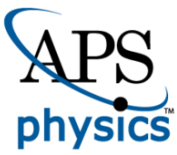

Extracting Entanglement Geometry from Quantum States

Katharine Hyatt, James R. Garrison, and Bela Bauer

Phys. Rev. Lett. **119**, 140502 — Published 2 October 2017

DOI: 10.1103/PhysRevLett.119.140502

Extracting entanglement geometry from quantum states

Katharine Hyatt,[1] James R. Garrison,[2,1] and Bela Bauer[3]

[1] *Department of Physics, University of California, Santa Barbara, California 93106, USA*
[2] *Joint Quantum Institute and Joint Center for Quantum Information and Computer Science, National Institute of Standards and Technology and University of Maryland, College Park, Maryland 20742, USA*
[3] *Station Q, Microsoft Research, Santa Barbara, California 93106, USA*

Tensor networks impose a notion of geometry on the entanglement of a quantum system. In some cases, this geometry is found to reproduce key properties of holographic dualities, and subsequently much work has focused on using tensor networks as tractable models for holographic dualities. Conventionally, the structure of the network – and hence the geometry – is largely fixed *a priori* by the choice of tensor network ansatz. Here, we evade this restriction and describe an unbiased approach that allows us to extract the appropriate geometry from a given quantum state. We develop an algorithm that iteratively finds a unitary circuit that transforms a given quantum state into an unentangled product state. We then analyze the structure of the resulting unitary circuits. In the case of non-interacting, critical systems in one dimension, we recover signatures of scale invariance in the unitary network, and we show that appropriately defined geodesic paths between physical degrees of freedom exhibit known properties of a hyperbolic geometry.

Tensor networks have proven to be a powerful and universal tool to describe quantum states. Originating as variational ansatz states for low-dimensional quantum systems, they have become a common language between condensed matter and quantum information theory. More recently, the realization that some key properties of holographic dualities [1–5] are reproduced in certain classes of tensor network states (TNS) [6, 7] has led to new connections to quantum gravity. In particular, many questions about holographic dualities appear more tractable in TN models [8–18]. The study of the geometry of TN states underlies these developments. Here, the physical legs of the network represent the boundary of some emergent "holographic" space that is occupied by the TN. While in networks such as matrix-product states (MPS) [19–21] and projected entangled-pair states (PEPS) [22–24] this space just reflects the physical geometry, other networks – such as the multi-scale entanglement renormalization ansatz (MERA) [25, 26] – can have non-trivial geometry in this space [7]. We will refer to this geometry as "entanglement geometry".

In this paper, we investigate whether this entanglement geometry can be extracted from a given quantum state without pre-imposing a particular structure on the TN [27]. We first describe a greedy, iterative algorithm that, given a quantum state, finds a 2-local unitary circuit that transforms this state into an unentangled (product) state (see Fig. 1). Such circuits, composed from unitary operators acting on two sites (which are not necessarily spatially close to each other), can be viewed as a particular class of TNS where the tensors are the unitary operators that form the circuit.

We then develop a framework for analyzing the geometry of these circuits. First, we introduce a locally computable notion of distance between two points in the circuit, thus inducing a geometry in the bulk. We then focus on a particular property of this geometry, the length of geodesics (shortest paths through the circuit) between physical (boundary) sites. A similar quantity has been previously discussed as a diagnostic of geometry in tensor networks [7], and reveals similar information as the minimal spanning surface in the celebrated Ryu-Takayanagi (RT) formula for the entanglement entropy in AdS/CFT [28, 29]. Crucially, our definition takes into account the strength of each local tensor, and thus allows us to numerically compute an appropriate length without imposing additional restrictions on the tensors [11] or *a priori* knowledge of the emergent geometry.

Applying these techniques to many-particle quantum states, we observe three regimes: (i) a flat (zero curvature) two-dimensional geometry, (ii) a hyperbolic two-dimensional geometry, and (iii) a geometry where the geodesic distance between all points is equal, which corresponds to zero (fractal) dimension. We first observe these in eigenstates of non-interacting fermions in a disorder potential. For low-energy eigenstates with weak disorder, we find a hyperbolic geometry and thus recover key aspects of the AdS/CFT duality [1–5]. Going beyond eigenstates, we study a quench from the localized to the delocalized regime, i.e. the evolution of a localized initial state under a Hamiltonian with vanishing disorder potential. In this case, the geodesics reveal detailed information about the deformation of the emergent geometry, which progresses from flat geometry (i) to zero-dimensional (iii). This process reproduces certain aspects of previous holographic analyses of quantum quenches [30–32].

In a complementary approach [33], we also examine the nature of emergent light cones in the unitary network. In the case of critical systems, these are found to exhibit features of scale invariance. In the cases of localized and thermal states, the light cones reveal that the entanglement is fully encoded in local and global operators, respectively.

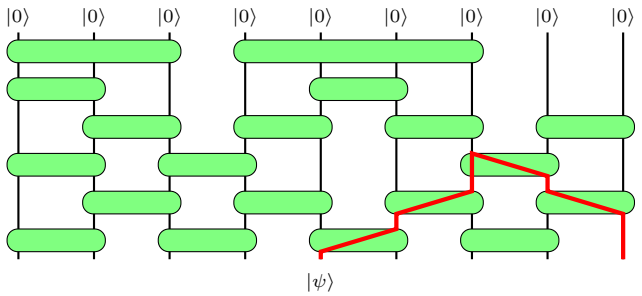

FIG. 1. Example of a two-local unitary circuit, where each unitary acts only on the two qubits that are at its ends. The thick red line indicates a geodesic between the 5th and 9th qubit (from the left), following a path through the circuit as given by Fig. 2.

Disentangling algorithm— Our algorithm for finding a unitary disentangling circuit is in many ways inspired by the strong-disorder renormalization group [34, 35]. However, there are two crucial differences. First, instead of acting on the Hamiltonian, the algorithm acts on a particular state. Second, rather than on the energetically strongest bond, at each step the algorithm works on the most strongly entangled pair of sites. The algorithm has two desirable properties. First, it works for a broad class of input states, including states that have area law and volume law entanglement. This comes at the cost of generating circuits that cannot in general be contracted in polynomial time. Second, each iteration of the iterative algorithm is completely determined by the output of the previous iteration; we thus avoid solving the challenging non-linear optimization problems that are usually encountered when optimizing a tensor network. Similar algorithms have been put forward in Refs. 17 and 36.

We take as input a quantum state $|\psi\rangle$ on a lattice $\mathcal{L}$. We denote as ρ_{ij} the reduced density matrix on sites $i, j \in \mathcal{L}$, $\rho_{ij} = \mathrm{Tr}_{\mathcal{L}\setminus\{i,j\}} |\psi\rangle\langle\psi|$, and as ρ_i the reduced density matrix on site i, $\rho_i = \mathrm{Tr}_{\mathcal{L}\setminus\{i\}} |\psi\rangle\langle\psi|$, and $S(\rho) = -\mathrm{Tr}\,\rho\log\rho$. The algorithm proceeds as follows:

Algorithm 1 *(i) Calculate the mutual information between all pairs of sites, $I(i:j) = I(\rho_{ij}) \equiv S(\rho_i) + S(\rho_j) - S(\rho_{ij})$, and find the pair (i,j) with the largest mutual information. If all $I(i:j)$ are below some predefined threshold ϵ, terminate. (ii) Find the unitary matrix $\hat{U}_{ij}$ that acts only on sites i and j and maximally reduces the amount of mutual information between these sites, i.e. solve $\min_{\hat{U}_{ij}} I(\hat{U}_{ij}\rho_{ij}\hat{U}_{ij}^\dagger)$. (iii) Set $|\psi\rangle \leftarrow \hat{U}_{ij}|\psi\rangle$, and return to step 1.*

Details of the algorithm, in particular step (ii), can be found in the Supplementary Material [33]. For an exact representation of a many-body state in a Hilbert space of dimension $\dim\mathcal{H}$, one iteration of the above algorithm can be carried out with computational cost $\mathcal{O}(L\dim\mathcal{H})$ [37]. For a system of non-interacting fermions, however, the algorithm can be completely expressed in terms of the correlation matrix $C_{ij} = \langle\hat{c}_i^\dagger\hat{c}_j\rangle$ [33, 38–40]. Given the initial correlation matrix, the algorithm can be performed in $\mathcal{O}(L)$ operations per iteration, where L is the number of fermionic modes. In all cases, a single iteration of the algorithm can be performed as fast or faster than finding the eigenstates. The number of iterations required to converge to an unentangled state depends heavily on the input state: for weakly entangled states, convergence is fast, while for states with large entanglement, such as completely random quantum states, convergence can be very slow. Furthermore, the algorithm is not straightforwardly applicable to certain specific classes of states (see, e.g., the perfect tensors of Ref. 11). We numerically explore convergence for some relevant cases in the Supplemental Material [33].

The algorithm ultimately constructs a unitary circuit $\hat{U} = \hat{U}^{(\tau)}_{i_\tau j_\tau}\ldots\hat{U}^{(2)}_{i_2 j_2}\hat{U}^{(1)}_{i_1 j_1}$ acting on the initial state $|\Psi\rangle$, where $\hat{U}^{(\tau)}_{i_\tau j_\tau}$ is the unitary obtained in the τ'th step. The number of execution steps corresponds to the number of unitaries comprising the circuit. The circuit is 2-local in the sense that each unitary acts on two sites, but it is *not* local in the lattice geometry because the two sites i and j may be arbitrarily far apart. Furthermore, this circuit is not unique: an ambiguity arises since the unitary can always be followed by a swap of the two sites or a single-site unitary while keeping the mutual information the same [33].

Emergent geometry of unitary circuits— A powerful way to probe the geometry of the unitary network is to measure the length of "geodesics", i.e. the shortest paths connecting two physical sites on the boundary of the circuit through the bulk of the circuit (see Fig. 1). The crucial ingredient for a numerical analysis of the unitary circuits is an appropriate notion of length for a path in the circuit which incorporates the strength of each unitary operator. It is obvious that a careful definition of this quantity is necessary: If, for example, one were simply to count the number of unitaries traversed in connecting two sites, one would – for a sufficiently deep circuit – always find a length of 1, since eventually all pairs of sites will be directly connected by a unitary. However, deep in the circuit the unitaries are very close to the identity, and therefore do not mediate correlations between the two sites. It is also desirable for the definition of length to be invariant under trivial deformations of the circuit, such as introducing additional swap, identity, or single-qubit gates. Finally, the distance measure should be computable locally and not rely on any global features of the graph.

Our definition of length builds on a local connection between geodesic length and correlations [8]. We construct a weighted, undirected graph as illustrated in Fig. 2: The vertices of the graph are the indices of the unitary operators. Edges connecting different operators

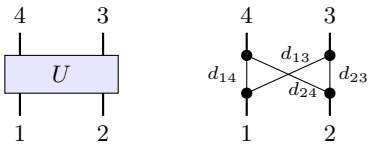

FIG. 2. *Left panel:* Labeling of the input and output indices on a unitary operator. *Right panel:* Local graph corresponding to the unitary operator, with weights labeled on the internal edges.

have weight 0, while the internal edges connecting different indices of the unitary have lengths d_{ab} as labeled in the right-hand side of Fig. 2. To define d_{ab}, we interpret the unitary as a wavefunction on four qubits and set $d_{ab} = -\log[I(a:b)/(2\log 2)]$, where $I(a:b)$ is the mutual information between qubits a and b of the normalized wavefunction. Unitarity dictates $d_{12} = d_{34} = \infty$: these two lengths are not included in the graph. Entanglement monogamy [41, 42] implies that if $d_{24} = 0$ ($d_{14} = 0$), d_{13} (d_{23}) must also vanish and d_{14} (d_{24}) must be infinite. Given this weighted, undirected graph, the minimal distance between two vertices is computable using standard graph algorithms.

To develop some intuition for this quantity, consider the length of a path in well-known TNS such as MPS/PEPS and MERA [7]. Assuming that each tensor in such a network has roughly equal strength, we can for now simply take the length to be the number of tensors that a path between two points traverses. For an MPS or PEPS, the length of the geodesic is then simply the physical distance between the sites, indicative of a flat entanglement geometry. In contrast, the length of a geodesic in a MERA scales only logarithmically with the physical distance, since the path is shorter when moving through the bulk of the TN [7]; this is a signature of a hyperbolic entanglement geometry.

It is important to contrast the geodesics considered here with the minimal surfaces in the RT formula for the holographic entanglement entropy. In the standard translation to TNS, such a minimal surface is given by the minimal number of bonds that need to be cut in order to completely separate two regions of physical sites. A minimal surface in this sense can be defined for any TN, and always yields an upper bound to the entanglement entropy between the two regions [43]. While in some cases these minimal surfaces also take the form of geodesics [11], they are distinct from the geodesics as defined in this manuscript, which *connect* pairs of sites rather than *separate* regions of sites. The difference is most easily seen in a MPS: while our geodesics are *linear* in the physical distance, the minimal separating surface is *constant*, since at most two bonds need to be cut to separate the TN. While our definition is more natural in the context of unitary circuits, they are complementary to each other, and both reveal similar information when appropriately interpreted.

It is important to recognize that while our distance measure locally is connected to correlations, there is no simple one-to-one correspondence between the behavior of our geodesics and the behavior of two-point correlation functions. As outlined in Ref. 7, an intuitive relation is for correlations to decay exponentially with the geodesic length. This relation is precise for MPS, and also suggests the possibility of power-law decay of correlations in MERA (although for certain MERA the correlations may decay faster). However, the connection breaks down in the case of a PEPS: while the length of a geodesic is always at least the physical (Manhattan) distance, it is possible to find PEPS whose correlations decay as a power law [44]. Finally, the intricate behavior in a quantum quench discussed below is largely invisible to two-point correlations.

Models— We first study the properties of the disentangling circuits in a model of non-interacting spinless fermions in one dimension moving in a disorder potential. We discuss further examples in the Supplemental Material [33]. The random-potential model is given by

$$\hat{H} = -t\sum_i \left(\hat{c}_i^\dagger \hat{c}_{i+1} + \hat{c}_{i+1}^\dagger \hat{c}_i\right) + \sum_i w_i \hat{c}_i^\dagger \hat{c}_i, \qquad (1)$$

where $\hat{c}_i^\dagger$ creates a spinless fermion on the i'th site of a chain of length L. Throughout this paper, we work with periodic boundary conditions, set $t = 1$ as an overall energy scale, and focus on Slater determinants at half filling. The random on-site potential is chosen from a uniform distribution of width W, $w_i \in [-W/2, W/2]$. For vanishing disorder $W \to 0$, this system is critical and the long-wavelength limit of the ground state is described by a free-boson conformal field theory with central charge $c = 1$. For any finite strength of the disorder potential, the fermions localize [45]. However, for very small $W \ll 1$, the localization length ξ_{loc} is large compared to the system sizes we study, allowing us to break translational invariance without significantly affecting physically observable properties.

Numerical results— Our numerical findings for the scaling with the physical distance of geodesics in ground states of (1) are shown in Fig. 3 for different disorder strengths. Consider first the case of very large disorder strength, and thus short localization length. The geodesic length initially grows as $d_g \sim \log d_p$ with the physical distance d_p (see in particular the inset of Fig. 3), and then crosses over to a linear dependence $d_g \sim d_p$, indicated by the sharp kink in Fig. 3. This behavior at large physical distance is characteristic of the flat entanglement geometry expected in a localized state. As the disorder strength decreases, the crossover shifts to larger and larger distances, indicating that the crossover length corresponds to the localization length. For very weak disorder potential (such as $W = 0.1$, where the localization

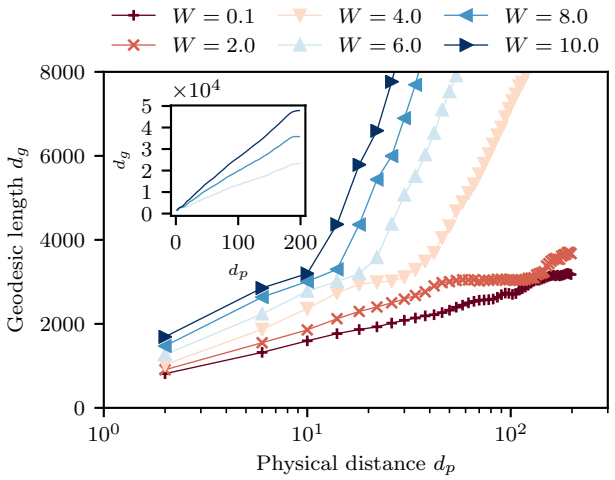

FIG. 3. Geodesic length of the $L = 500$ Anderson disorder model for different values of the disorder strength W, with 200 realizations each. While the physical distance is given in lattice spacings, the geodesic length is in arbitrary units. The inset shows the same data for $W = 6.0, 8.0, 10.0$ on a linear scale to highlight the linear dependence $d_g \sim d_p$.

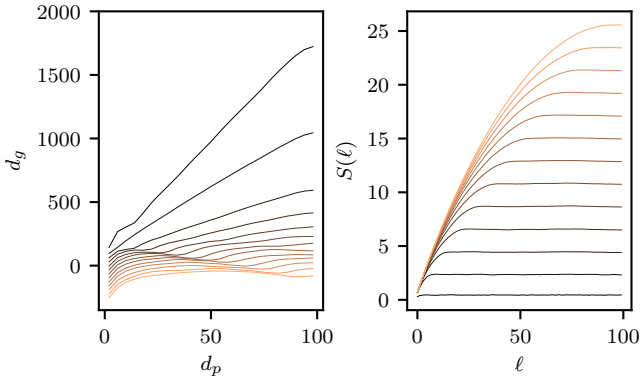

FIG. 4. Quench from the ground state of the Anderson disorder model with with $L = 200$ sites and $W = 8$ to the clean case $W = 0$. *Left panel:* Geodesic length d_g as a function of physical distance d_p. *Right panel:* entanglement entropy of a contiguous region of ℓ sites. Individual lines represent snapshots of the system at times equally spaced between $T = 0$ to $T = 25.25$ averaged over 200 disorder realizations. The curves in the left panel have been offset by $-15 \cdot T$. Increasing copper/decreasing blackness indicates times further in the quench.

length exceeds the system size), the region of logarithmic dependence spans the entire system. This is the hallmark feature of hyperbolic entanglement geometry and establishes a connection to other holographic mappings, such as the AdS/CFT correspondence.

Going beyond eigenstates, we now consider a quench where the system is initialized in the ground state of (1) with finite disorder ($W = 8$ in the examples chosen here), and is subsequently evolved under the translationally-invariant Hamiltonian ($W = 0$). This is similar to quenching the mass gap from a finite value to zero. We evolve up to time $T = 100$, performing the disentangling algorithm to obtain $d_g(d_p)$ at various times during the quench. Our results are shown in the left panel of Fig. 4, while the right panel shows the growth of bipartite entropy of a block of ℓ sites, and thus the crossover from area-law to volume-law entanglement entropy scaling. Note that here, in contrast to Fig. 3, the horizontal axis scales linearly.

Initially, the system exhibits the expected $d_g \sim d_p$ scaling of a localized system. The dominant effect at early times is a fast reduction in the scaling coefficient. However, careful examination at early times already reveals a drastic change in the scaling behavior at short distances, where d_g, instead of growing linearly with d_p, becomes nearly constant (or even decreases slightly). There is a sharp kink associated with the crossover from this to the linear behavior, which moves out to larger and larger distances with time, and finally reaches the maximal distance $d_p = L/2$. Comparison with the right panel of Fig. 4 shows that the location of the kink corresponds to the crossover from area-law to volume-law scaling of the bipartite entanglement entropy. Once the system has reached a long-time state with volume-law entanglement entropy, d_g shows some d_p-dependence only for short distances, and is flat otherwise.

In terms of the emergent entanglement geometry, the interpretation of these findings is as follows: the global quench excites a homogeneous and finite density of local excitations, which ballistically spread and entangle with each other. Both the kink and the area- to volume-law crossover follow the spread of this wavefront. For distances beyond this (time-dependent) scale, the circuit is not *qualitatively* affected; however, a *quantitative* change in the coefficient d_g/d_p occurs. Similar to the coefficient of an area law, this quantity is easily changed by a local finite-depth unitary. Within the characteristic length scale, on the other hand, the nature of the circuit is qualitatively changed from a short-ranged circuit encoding an area law state to a very long-ranged circuit, with unitaries connecting the current location of an excitation to its origin, and thus encoding volume-law entanglement. In the final state, this long-ranged circuit dominates the geodesic, with only the short-distance behavior which originates from the boundary of the circuit exhibiting some locality. This bears resemblance to the final state in other holographic theories of quantum quenches [30, 31], with the non-local part of the circuit playing the role of a black hole. The relation of our results for intermediate times to the model put forward in these references is an open question left for future work. We also note that some details of the emergent geometry, including in particular oscillations observed at times longer than the initial spreading of entanglement shown in Fig. 4, may be due to integrability of the model.

Outlook— While we have so far applied our methods

to systems where a holographic description is already known, the fact that we did not make use of any *a priori* knowledge of these systems makes our methods ideally suited to systems with no known holographic description. Most prominently, this includes the many-body localization transition [46–51], which is known to be characterized through entanglement properties [50] while the details of the transition remain controversial [52–54].

We thank M. P. A. Fisher, G. Refael and J. Sonner for insightful discussions, and A. Antipov and S. Fischetti for comments on earlier drafts of this manuscript. JRG was supported by the NIST NRC Research Postdoctoral Associateship Award, by the National Science Foundation under Grant No. DMR-14-04230, and by the Caltech Institute of Quantum Information and Matter, an NSF Physics Frontiers Center with support of the Gordon and Betty Moore Foundation. This material is based upon work supported by the National Science Foundation Graduate Research Fellowship under Grant No. DGE 1144085. Any opinion, findings, and conclusions or recommendations expressed in this material are those of the authors(s) and do not necessarily reflect the views of the National Science Foundation. We acknowledge support from the Center for Scientific Computing at the CNSI and MRL: an NSF MRSEC (DMR-1121053) and NSF CNS-0960316. This work was in part performed at the Aspen Center for Physics, which is supported by National Science Foundation grant PHY-1066293.

[1] G. 't Hooft, (1993), arXiv:gr-qc/9310026.
[2] L. Susskind, Journal of Mathematical Physics **36**, 6377 (1995).
[3] J. Maldacena, International Journal of Theoretical Physics **38**, 1113 (1999).
[4] E. Witten, Adv. Theor. Math. Phys. **2**, 253 (1998), arXiv:hep-th/9802150.
[5] O. Aharony, S. S. Gubser, J. Maldacena, H. Ooguri, and Y. Oz, Physics Reports **323**, 183 (2000).
[6] B. Swingle, Phys. Rev. D **86**, 065007 (2012).
[7] G. Evenbly and G. Vidal, Journal of Statistical Physics **145**, 891 (2011).
[8] X.-L. Qi, Preprint (2013), arXiv:1309.6282.
[9] C. Bény, New Journal of Physics **15**, 023020 (2013).
[10] A. Mollabashi, M. Naozaki, S. Ryu, and T. Takayanagi, Journal of High Energy Physics **2014**, 98 (2014).
[11] F. Pastawski, B. Yoshida, D. Harlow, and J. Preskill, Journal of High Energy Physics **2015**, 1 (2015).
[12] N. Bao, C. Cao, S. M. Carroll, A. Chatwin-Davies, N. Hunter-Jones, J. Pollack, and G. N. Remmen, Physical Review D **91**, 125036 (2015).
[13] M. Miyaji and T. Takayanagi, Progress of Theoretical and Experimental Physics **2015**, 073B03 (2015), arXiv:1503.03542 [hep-th].
[14] B. Czech, L. Lamprou, S. McCandlish, and J. Sully, Journal of High Energy Physics **2016**, 100 (2016).
[15] P. Hayden, S. Nezami, X.-l. Qi, N. Thomas, M. Walter, and Z. Yang, Journal of High Energy Physics **2016**, 1 (2016).
[16] Z. Yang, P. Hayden, and X.-L. Qi, Journal of High Energy Physics **2016**, 1 (2016).
[17] S. Kehrein, Preprint (2017), arXiv:1703.03925.
[18] X.-L. Qi, Z. Yang, and Y.-Z. You, Preprint (2017), arXiv:1703.06533.
[19] M. Fannes, B. Nachtergaele, and R. F. Werner, Communications in Mathematical Physics **144**, 443 (1992).
[20] S. R. White, Phys. Rev. Lett. **69**, 2863 (1992).
[21] S. Östlund and S. Rommer, Phys. Rev. Lett. **75**, 3537 (1995).
[22] A. Gendiar, N. Maeshima, and T. Nishino, Progr. Theor. Phys. **110**, 691 (2003).
[23] T. Nishino, Y. Hieida, K. Okunushi, N. Maeshima, Y. Akutsu, and A. Gendiar, Progr. Theor. Phys. **105**, 409 (2001).
[24] F. Verstraete and J. I. Cirac, Preprint (2004), arXiv:cond-mat/0407066.
[25] G. Vidal, Phys. Rev. Lett. **99**, 220405 (2007).
[26] G. Vidal, Phys. Rev. Lett. **101**, 110501 (2008).
[27] C. Cao, S. M. Carroll, and S. Michalakis, Phys. Rev. D **95**, 024031 (2017), arXiv:1606.08444 [hep-th].
[28] S. Ryu and T. Takayanagi, Phys. Rev. Lett. **96**, 181602 (2006).
[29] S. Ryu and T. Takayanagi, Journal of High Energy Physics **2006**, 045 (2006).
[30] V. E. Hubeny, M. Rangamani, and T. Takayanagi, Journal of High Energy Physics **2007**, 062 (2007).
[31] J. Abajo-Arrastia, J. Aparício, and E. López, Journal of High Energy Physics **2010**, 149 (2010).
[32] J. Sonner, A. Del Campo, and W. H. Zurek, Nature Communications **6**, 7406 (2015), arXiv:1406.2329 [hep-th].
[33] See Supplemental Material for details on light cone growth and the disentangling algorithm, which includes Refs. [55–65].
[34] S.-K. Ma, C. Dasgupta, and C.-K. Hu, Phys. Rev. Lett. **43**, 1434 (1979).
[35] D. S. Fisher, Phys. Rev. B **50**, 3799 (1994).
[36] C. Chamon, A. Hamma, and E. R. Mucciolo, Physical review letters **112**, 240501 (2014).
[37] Note that while the first iteration is carried out in $\mathcal{O}(L^2 \dim \mathcal{H})$ time, all subsequent iterations can be carried out in $\mathcal{O}(L \dim \mathcal{H})$ time, as only quantities involving the transformed sites i and j must be recalculated.
[38] G. Vidal, J. I. Latorre, E. Rico, and A. Kitaev, Phys. Rev. Lett. **90**, 227902 (2003).
[39] I. Peschel, Journal of Physics A: Mathematical and General **36**, L205 (2003).
[40] I. Peschel and V. Eisler, Journal of Physics A: Mathematical and Theoretical **42**, 504003 (2009).
[41] V. Coffman, J. Kundu, and W. K. Wootters, Phys. Rev. A **61**, 052306 (2000).
[42] B. M. Terhal, IBM Journal of Research and Development **48**, 71 (2004).
[43] This well-known fact is discussed explicitly e.g. in Refs. 7, 44, and 66.
[44] F. Verstraete, M. M. Wolf, D. Perez-Garcia, and J. I. Cirac, Phys. Rev. Lett. **96**, 220601 (2006).
[45] P. W. Anderson, Phys. Rev. **109**, 1492 (1958).
[46] D. M. Basko, I. L. Aleiner, and B. L. Altshuler, Annals of Physics **321**, 1126 (2006).

[47] V. Oganesyan and D. A. Huse, Phys. Rev. B **75**, 155111 (2007).
[48] A. Pal and D. A. Huse, Phys. Rev. B **82**, 174411 (2010).
[49] J. H. Bardarson, F. Pollmann, and J. E. Moore, Phys. Rev. Lett. **109**, 017202 (2012).
[50] B. Bauer and C. Nayak, J. Stat. Mech: Theor. Exp. **9**, 09005 (2013), arXiv:1306.5753 [cond-mat.dis-nn].
[51] D. J. Luitz, N. Laflorencie, and F. Alet, Phys. Rev. B **91**, 081103 (2015).
[52] T. Grover, Preprint (2014), arXiv:1405.1471.
[53] V. Khemani, S. P. Lim, D. N. Sheng, and D. A. Huse, Preprint (2016), arXiv:1607.05756.
[54] X. Yu, D. J. Luitz, and B. K. Clark, Phys. Rev. B **94**, 184202 (2016).
[55] K. Modi, T. Paterek, W. Son, V. Vedral, and M. Williamson, Phys. Rev. Lett. **104**, 080501 (2010).
[56] K. Modi, A. Brodutch, H. Cable, T. Paterek, and V. Vedral, Rev. Mod. Phys. **84**, 1655 (2012).
[57] M. Srednicki, Phys. Rev. Lett. **71**, 666 (1993).
[58] C. Callan and F. Wilczek, Physics Letters B **333**, 55 (1994).
[59] C. Holzhey, F. Larsen, and F. Wilczek, Nuclear Physics B **424**, 443 (1994).
[60] G. Refael and J. E. Moore, Phys. Rev. Lett. **93**, 260602 (2004).
[61] S. Aubry and G. André, Ann. Israel Phys. Soc **3**, 18 (1980).
[62] S. Iyer, V. Oganesyan, G. Refael, and D. A. Huse, Phys. Rev. B **87**, 134202 (2013).
[63] P. Zanardi, Phys. Rev. A **63**, 040304 (2001).
[64] X. Wang, B. C. Sanders, and D. W. Berry, Phys. Rev. A **67**, 042323 (2003).
[65] V. Vedral, M. B. Plenio, M. A. Rippin, and P. L. Knight, Phys. Rev. Lett. **78**, 2275 (1997).
[66] S. X. Cui, M. H. Freedman, O. Sattath, R. Stong, and G. Minton, Journal of Mathematical Physics **57**, 062206 (2016).